

# Advancing solar energy harvesting: Artificial intelligence approaches to maximum power point tracking

Meriem Boudouane<sup>1</sup>, Lahoussine Elmahni<sup>1</sup>, Rachid Zriouile<sup>1</sup>, Soufyane Ait El Ouahab<sup>2</sup>

<sup>1</sup>Materials and Renewable Energy Laboratory, Physics Department, University of Ibn Zohr, Agadir, Morocco

<sup>2</sup>Methodology and Information Processing Laboratory, Physics Department, University of Ibn Zohr, Agadir, Morocco

## Article Info

### Article history:

Received Jun 4, 2024

Revised Oct 27, 2024

Accepted Nov 28, 2024

### Keywords:

Boost converter  
Conventional methods  
Intelligent methods  
Modeling  
MPPT control  
PV generator

## ABSTRACT

This paper presents a comparative study of five maximum power point tracking (MPPT) control techniques in photovoltaic (PV) systems. The algorithms evaluated include classical methods, such as perturb and observe (P&O) and incremental conductance (IC), as well as intelligent approaches such as fuzzy logic (FL), artificial neural networks (ANNs), and adaptive neuro-fuzzy inference system (ANFIS). Intelligent methods provide faster response times and fewer oscillations around the maximum power point (MPP). The structure of the PV system includes a PV generator, load, and DC/DC boost converter driven by an MPPT controller. The performance of these techniques is analyzed under identical climatic conditions (same irradiation and temperature) in terms of efficiency, response time, response curve, accuracy in tracking the MPP, and others considered in this work. Simulations were performed using MATLAB-Simulink software, demonstrating that ANNs and ANFIS outperform traditional methods in dynamic environments, with FL being computationally intensive. P&O exhibited significant oscillations, while IC showed slower tracking speed.

*This is an open access article under the [CC BY-SA](#) license.*



## Corresponding Author:

Meriem Boudouane

Materials and Renewable Energy Laboratory, Physics Department, Faculty of Sciences-Agadir

University Ibn Zohr

BP 32/S, CP 80000, Agadir, Morocco

Email: meriemprof@gmail.com

## 1. INTRODUCTION

Global energy demand continues to rise, traditionally relying on fossil fuels due to their high energy potential. However, the depletion of these resources and their contribution to greenhouse gas emissions has prompted the search for alternative energy sources. Renewable energy, particularly photovoltaic (PV), offers a sustainable and environmentally friendly solution. PV systems harness solar energy to generate electricity. Still, their efficiency highly depends on the system's ability to track the maximum power point (MPP), which varies with changing climatic conditions, such as solar irradiance and temperature. Maximum power point tracking technology is crucial for optimizing the power output of PV systems. With its ability to adjust maximum power point in real time, MPPT significantly improves the performance of photovoltaic installations, boosting efficiency and profitability. The purpose of MPPT is to track and extract the maximum available power from the PV module by adjusting its electrical operating point. To accomplish this, a DC/DC converter with an MPPT controller is installed between the PV generator and load to adapt its resistance by adjusting the duty cycle converter. Many MPPT approaches are utilized to operate PV systems at maximum power.

In review, various MPPT methodologies were suggested to extract the maximum power from the PV

generators. The classical MPPT algorithms were relatively simple and easy to implement, such as fractional short circuit current (OSC) [1], [2], fractional open circuit voltage (OCV) [3]-[5], perturbation and observation (PO) [6], [7], incremental conductance (IC) [8]-[10], and hill-climbing (HC) [11], [12]. Despite their simplicity and gains in development, these techniques have limitations, most notably a slower response time, notable oscillates around maximum power point in steady states, and low efficiency during rapid weather variations.

Nowadays, more sophisticated and intelligent techniques offer substantial advantages over classical methods, such as simple implementation, the capacity to follow the MPP under whether operating conditions, and faster convergence. These include metaheuristic algorithms, particle swarm optimization (PSO) [13], ant colony (AC) [14], artificial bee colony (ABC) [15], herd horse optimization (HHO) [16], cuckoo search (CS) [17], and grey wolf optimization (GWO) [18] among others. These new approaches have improved response time and systems oscillation; their main challenge is population initialization. Other intelligent approaches that have proven robust in MPPT control, such as fuzzy logic (FL) [19]-[21], artificial neural networks (ANNs) [22]-[24], and adaptive neuro-fuzzy inference system (ANFIS) [21], [25], these techniques necessitate system learning expertise and a database.

The goal of this paper is to conduct a comparative analysis of the efficiency of MPPT tracking using conventional perturbation and observation (P&O) and incremental conductance (IC) techniques, as well as artificial fuzzy logic (FL), artificial neural networks (ANNs), and adaptive neuro-fuzzy inference system (ANFIS) techniques. The criteria for comparison implemented in this study include the convergence time of MPPT control, MPPT error, steady-state power oscillation, and effects on PV panel voltage ( $V_{pv}$ ) and current ( $I_{pv}$ ) due to irradiation and temperature variations. DC/DC boost converter is used as an interface between the PV generator and load.

The PV system proposed is simulated using MATLAB-Simulink software. Simulation results have proven that the best technique is the adaptive neuro-fuzzy inference system (ANFIS), outperforming other methods in MPPT controller performance, reducing the response time of PV systems, increasing efficiency, and eliminating oscillations. The outcomes of ANNs are very similar to those of ANFIS. The fuzzy logic technique (FL) produces good results, but its complex calculation system makes it take too long to compute. Despite their effectiveness in implementing MPP tracking for climate change, conventional methods exhibit oscillations around the maximum power point. The subsequent sections are organized as follows: i) Section 2 provides mathematical PV modeling; ii) Followed by an overview of the several MPPT approaches used in section 3; iii) Section 4 describes the suggested PV system; iv) The simulation results are provided and analyzed in section 5; and v) The document is concluded in section 6.

## 2. MATHEMATICAL PV MODELING

A PV panel mathematical model describes the electrical properties of a PV generator in terms of physical and environmental factors, such as solar irradiation and temperature. A single-diode model [26]-[28] shown in Figure 1 is commonly used to simulate photovoltaic panels, and is described by an equation that relates the current and voltage characteristics of the panel under varying weather conditions. The current produced by the PV cell,  $I_{pv}$ , is derived using Kirchhoff's current law, accounting for the photocurrent  $I_{ph}$ , the diode current  $I_d$ , and the shunt current  $I_{sh}$ . This relationship is given by (1).

$$I_{pv} = I_{ph} - I_d - I_{sh} \quad (1)$$

The (2) expresses photocurrent,  $I_{ph}$ , in terms of temperature and solar irradiation.

$$I_{ph} = [I_{sc} + K_i(T_{amb} - T_{ref})](G/G_{ref}) \quad (2)$$

Where  $I_{sc}$ : short circuit current under standard test conditions (STC), (1000 W/m<sup>2</sup>, 25 °C, AM1.5 spectrum);  $K_i$ : is the temperature coefficient of the cell;  $T_{amb}$  and  $T_{ref}$ : are working temperature and reference temperature in Kelvin respectively;  $G$  and  $G_{ref}$ : are working irradiance and reference irradiance respectively  $G_{ref} = 1000 \text{ W/m}^2$ .

The diode current is defined by (3).

$$I_d = I_s \left[ \exp\left(\frac{qV_d}{aKT}\right) - 1 \right] = I_s \left[ \exp\left(\frac{q(V_{pv} + R_s I_{pv})}{aKT}\right) - 1 \right] \quad (3)$$

Where,  $q$ : Electron charge ( $1.6 \cdot 10^{-19}$  C);  $K$ : Boltzmann constant ( $1.38 \cdot 10^{-23}$  Joules/Kelvin);  $a$ : Ideality factor; and  $T$ : PV temperature in Kelvin.

The diode saturation current  $I_s$ , can be determined using (4), where  $I_{rs}$  is the reverse saturation current given by (5), and the relationship with temperature is governed by the exponential term.

$$I_s = I_{rs} \cdot \left( \frac{T_{amb}}{T_{ref}} \right)^3 \exp \left[ \frac{qE_g \left( \frac{1}{T_{ref}} - \frac{1}{T_{amb}} \right)}{aK} \right] \quad (4)$$

$$I_{rs} = \frac{I_{sc}}{\exp \left( \frac{qV_{oc}}{N_s a K T} \right) - 1} \quad (5)$$

Where  $E_g$ : is the semiconductor bandgap energy=1.1 eV for  $S_i$ .

The (6) represents the shunt resistance current  $I_{sh}$ , which is found by the law of node.

$$I_{sh} = \frac{V_{pv} + R_s \cdot I_{pv}}{R_{sh}} \quad (6)$$

The final relation of cell current  $I_{pv}$  given in (7) can be obtained by substituting (3) and (6) in (1).

$$I_{pv} = I_{ph} - I_s \left[ \exp \left( \frac{q(V_{pv} + R_s I_{pv})}{aK T} \right) - 1 \right] - \frac{V_{pv} + R_s \cdot I_{pv}}{R_{sh}} \quad (7)$$

In order to increase the electricity produced by photovoltaic conversion, many cells are associated in series and parallel [29] as illustrated in Figure 2.  $N_s$  and  $N_p$  present the numbers of series and parallel cells. The current and voltage delivered by the PV array are expressed as in (8) and (9).

$$I_a = N_p \cdot I_{pv} \quad (8)$$

$$V_a = N_s \cdot V_{pv} \quad (9)$$

The photovoltaic array's current is given by (10).

$$I_a = N_p I_{ph} - N_p I_s \left[ \exp \left( \frac{q(V_a + \frac{N_s}{N_p} R_s I_a)}{N_s a K T} \right) - 1 \right] - \frac{V_a + \frac{N_s}{N_p} R_s I_a}{\frac{N_s}{N_p} R_{sh}} \quad (10)$$

The current-voltage characteristic of a solar panel describes the relationship between the current and voltage it produces shown in Figure 3. Several key electrical properties define a solar panel's performance, including open circuit voltage ( $V_{oc}$ ), short circuit current ( $I_{sc}$ ), and maximum power point (MPP). Solar panel output is affected by two main factors: solar irradiance and temperature. When solar irradiance decreases at a constant temperature of 25 °C, the panel output declines as shown in Figure 3(a). On the other hand, when the temperature rises at a constant irradiance of 1000 W/m<sup>2</sup>, the voltage decreases while the current remains steady as seen in Figure 3(b).

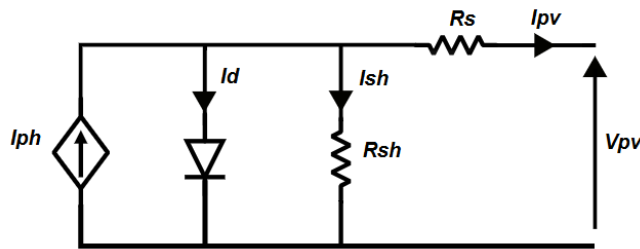


Figure 1. Solar cell circuit diagram

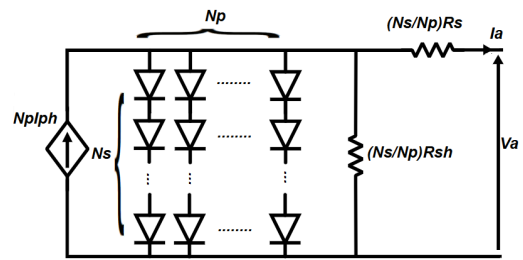


Figure 2. Solar PV array formation

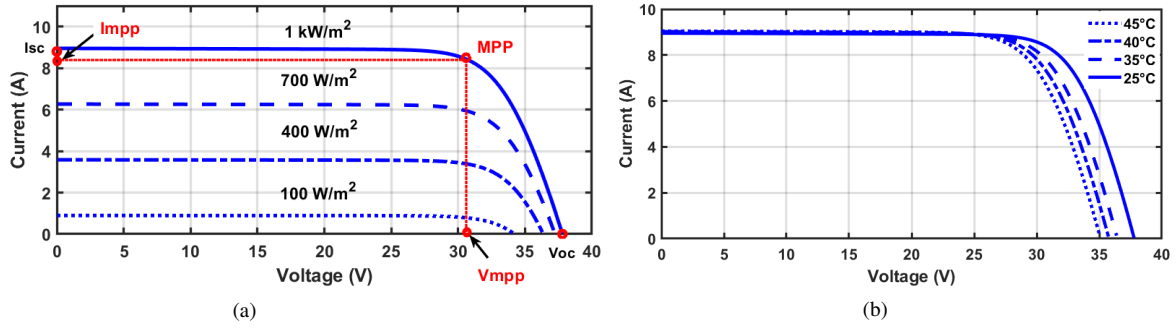


Figure 3.  $I_{pv}$ - $V_{pv}$  PV panel's characteristics: (a) with a steady temperature of 25 °C and (b) with a steady irradiation of 1000 W/m<sup>2</sup>

### 3. STRATEGIES FOR MAXIMUM POWER POINT TRACKING

#### 3.1. Maximum power point tracking (MPPT)

Figure 4 illustrates the power output of a PV panel as a function of the voltage at its terminals; this is distinguished by a peak in panel power output. Figures 4(a) and 4(b) indicate that MPP changes with weather conditions, so the MPPT approach is critical to keeping systems working at this optimum position. This sub-section presents five techniques developed in this work, enabling MPPT. MPPT commands developed are classical and intelligent. Classical perturbation and observation (P&O), incremental conductance (IC), intelligent fuzzy logic (FL), artificial neural networks (ANNs), and adaptive neuro-fuzzy inference system (ANFIS) methods are used first.

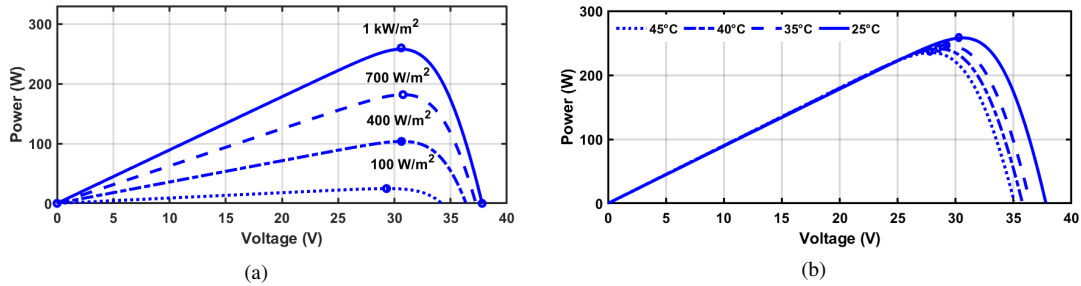


Figure 4.  $P_{pv}$ - $V_{pv}$  PV panel's characteristics: (a) with a steady temperature of 25 °C and (b) with a steady irradiation of 1000 W/m<sup>2</sup>

#### 3.2. Classical techniques

##### 3.2.1. Perturb and observe (P&O)

P&O is a commonly used approach to MPPT research, because it's simple and only requires voltage and current measures of PV generator  $V_{pv}$ ,  $I_{pv}$  [30], [31]. The flowchart of the P&O algorithm is illustrated in Figure 5. It operates with a fixed step size. This algorithm is based on perturbation of PV panel voltage, then calculates PV panel power  $P_{pv}(k)$  at time  $k$ , and compares it with previous time  $P_{pv}(k-1)$  which determines whether the derivative of power is positive or negative. A positive derivative means the operating point is approaching the MPP, the search direction is retained. When the operating point exceeds MPP, the power derivative becomes negative, and the search direction must be reversed to move back to MPP. The direction of searching defines whether the control is increasing or decreasing duty cycle  $D$ . At maximum power, the power derivative is null.

##### 3.2.2. Incremental conductance (IC)

The IC algorithm is also based on the variation of module power with voltage [10], [31]. The power variation is given by (11), solving this equation equal to zero at MPP as (12) shows, positive to the left according

to (13) and negative to the right of maximum according to (14). The flowchart of the IC algorithm is presented in Figure 6.

$$\frac{dP}{dV} = \frac{d(VI)}{dV} = I + \frac{VdI}{dV} = I + V \frac{\Delta I}{\Delta V} \quad (11)$$

From the relation above we find (12)-(14).

$$\frac{\Delta I}{\Delta V} = -\frac{I}{V} \quad \text{at MPP} \quad (12)$$

$$\frac{\Delta I}{\Delta V} > -\frac{I}{V} \quad \text{on MPP's left} \quad (13)$$

$$\frac{\Delta I}{\Delta V} < -\frac{I}{V} \quad \text{on MPP's right} \quad (14)$$

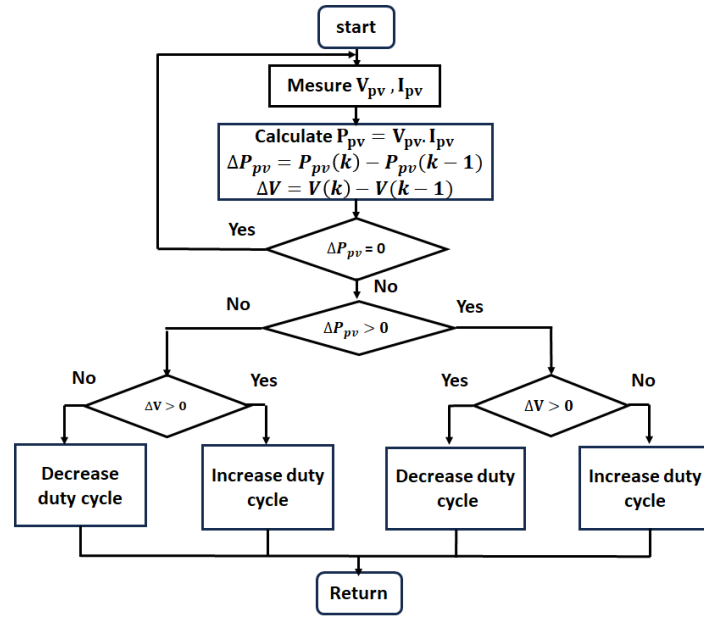


Figure 5. The P&O flowchart

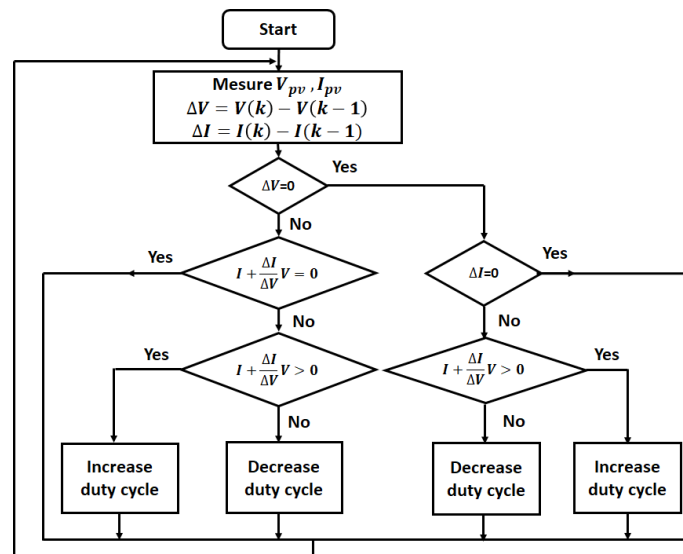


Figure 6. The IC flowchart

### 3.3. Intelligent techniques

#### 3.3.1. Fuzzy logic (FL)

FL is an artificial intelligence technique inspired by human reasoning formalism that introduces linguistic variables and rules. MPPT fuzzy controllers are implemented in three phases: fuzzification, inference, and defuzzification [21], [32]. Figure 7 shows the fuzzy controller structure.

Fuzzification is the transformation of numerical variables to fuzzy variables (linguistic variables) by associating truthfulness rules with them. In fuzzy inference, rules (and results) are constructed based on linguistic variables, each rule is assigned a truthfulness value, and the rules are then aggregated to obtain a single (linguistic) result. In defuzzification, a linguistic result is converted to a numerical result.

E is error represents the slope of the (P, V) curve and CE is variation of error, as provided by (15) and (16), respectively.

$$E(k) = \frac{\Delta P(k)}{\Delta V(k)} = \frac{P(k) - P(k-1)}{V(k) - V(k-1)} \quad (15)$$

$$CE(k) = E(k) - E(k-1) \quad (16)$$

Input linguistic variables are expressed as negative big (NB), negative small (NS), zero (Z), positive small (PS), and positive big (PB). The output variable is expressed as zero (Z), small (S), medium (M), big (B), and very big (VB). The following Table 1 presents a list of various rules employed in fuzzy controller. Then Figure 8 shows the structure of membership functions E, CE, and D.

		Table 1. Fuzzy control rules				
		CE				
E		NB	NS	Z	PS	PB
	NB	Z	Z	Z	B	M
	NS	Z	Z	S	M	B
	Z	Z	S	M	B	VB
	PS	S	M	B	VB	VB
	PB	M	B	VB	VB	VB

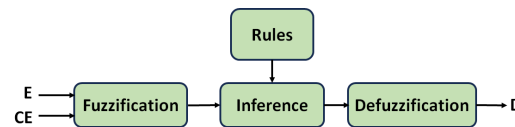


Figure 7. Fuzzy controller structure

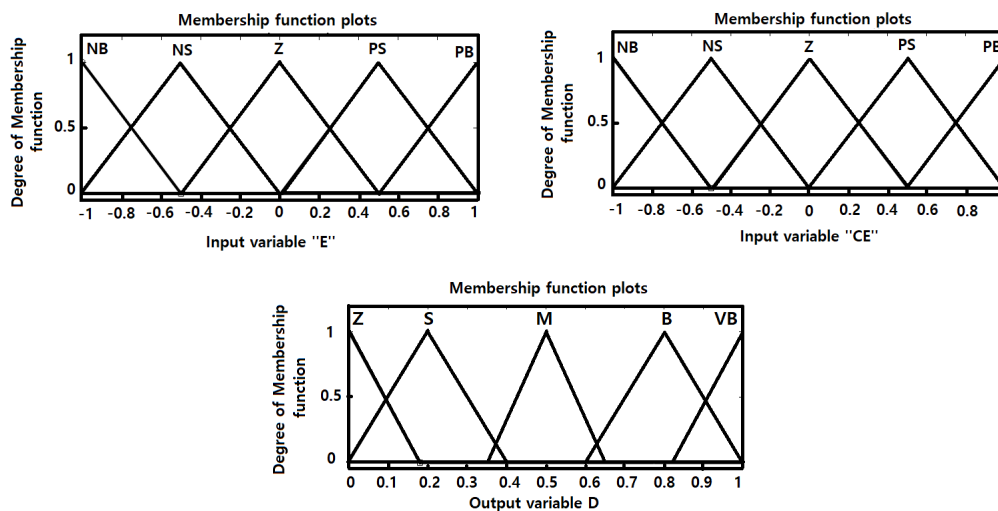


Figure 8. E(k), CE(k), and D membership functions

### 3.3.2. Artificial neural networks (ANNs)

ANNs are one of the most powerful artificial intelligence techniques. ANNs are inspired by the processing methodology of the human brain and have yielded the best results in many applications, including controlling MPPT in PV systems [33]-[35]. The basic element of the artificial neural network is the artificial neuron shown in Figure 9, which is a mathematical model of biological neuron. It's composed of three basic elements: a set of connections to various inputs  $x_i$  each with a weight  $\omega_i$ , a summator to calculate a linear combination of inputs  $x_i$  weighted by coefficients  $\omega_i$  expressed by (17), and an activation function  $f$  to delimit the neuron's output  $y$ .

$$S = \sum_{i=1}^n \omega_i \cdot x_i - \omega_0 \quad (17)$$

Neuron output  $y$  equals the activation function value given by (18). The activation functions commonly used are the Heaviside and Sigmoid function.

$$y = f\left(\sum_{i=1}^n \omega_i \cdot x_i - \omega_0\right) \quad (18)$$

Neural networks are structured by some nodes (neurons) interconnected by directional connections. Every node is a processing unit, with links representing causal relationships between nodes. The nodes are organized as layers, illustrated in Figure 10 input, hidden, and output layers [23], [24]. The ANNs principal task is the learning process, performed through an iterative process of adaptation of weights  $\omega_i$  to achieve optimal function output  $D$  for each input combination  $(G, T)$ .  $\omega_i$  values are randomly initialized and error-corrected between  $D_i$  values obtained and those expected.

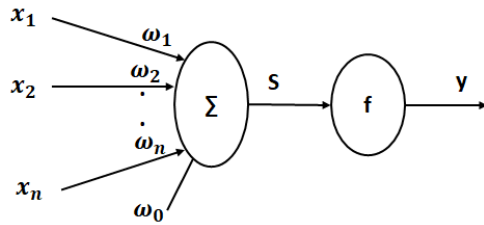


Figure 9. Artificial neuron structure

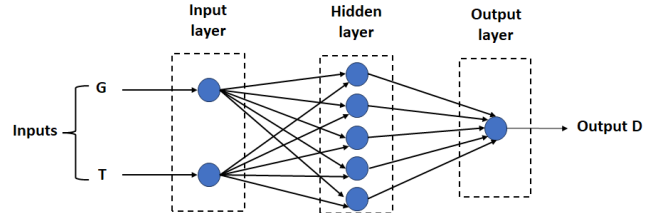


Figure 10. ANN structure

### 3.3.3. Adaptive neuro-fuzzy inference system (ANFIS)

ANFIS is an artificial neural network based on the fuzzy inference system. Combine the advantages of both complementary techniques neural network learning capability plus fuzzy logic flexibility and readability [21], [25]. ANFIS-MPPT controller is one of the strongest controllers for a PV system, featuring less fluctuations around MPP optimized point, fast tracking speed, and short computation time.

ANFIS Simulink model controller is presented in Figure 11(a). ANFIS adaptive network consists of a multi-layer network. Figure 11(b) illustrates the ANFIS controller structure used in this work, which is composed of five layers.

Layer 1 contains system inputs (irradiation  $G$ , temperature  $T$ ). Layer 2 "fuzzifies" inputs  $G$  and  $T$ . Each node in this layer calculates the membership degrees of input values using membership functions. Six triangular membership functions are used, three for irradiation and three for temperature, as illustrated in Figures 11(c) and 11(d). Layer 3 is a fuzzy rules layer. Layer 4 enables normalization and computes output rules. The output ("summing") layer contains a single neuron that provides the ANFIS output by summing the outputs of all defuzzification neurons.

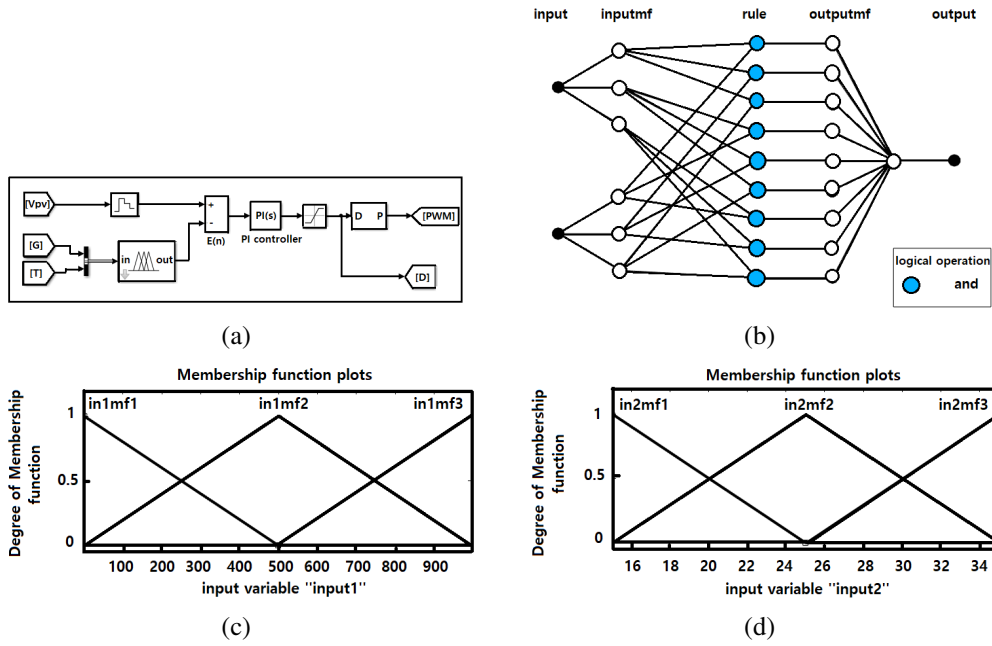


Figure 11. ANFIS: (a) Simulink model controller, (b) controller structure, (c) membership function of irradiation, and (d) membership function of temperature

#### 4. PROPOSED PV SYSTEM

The PV system recommended in this study is illustrated in Figure 12. It comprises a PV generator, resistor load, and DC/DC boost chopper driven by an MPPT controller. MPPT control is necessary to push the PV panel to run and extract maximum power under various weather situations. In this work, five distinct MPPT approaches were developed. The MPPT controller continuously receives voltage and current measurements from the PV generator and adjusts duty cycle  $D$  of the pulse width modulation (PWM) signal produced by the PWM generator. The system has been examined using MATLAB-Simulink.

##### 4.1. PV panel

In this research, the simulation is performed using an API-M260 PV module. This PV module is tested under various irradiance and temperature conditions. Table 2 lists the major technical specifications for this PV module.

##### 4.2. DC-DC boost chopper

A DC-DC chopper is an electronic power circuit that connects the PV generator to the load [36], [37]. The selected converter is the boost, the relationship between voltage and current input and output is determined by (19) and (20). Its main components are an inductor, two capacitors, and a transistor. A high-frequency switching signal (PWM) applied to the transistor gate controls power transfer between the PV generator and the load. The electrical parameters for the boost converter are shown in Table 3.

$$V_{out} = \frac{V_{pv}}{1 - D} \quad (19)$$

$$I_{pv} = \frac{I_{out}}{1 - D} \quad (20)$$

Where  $V_{pv}$  and  $V_{out}$  are PV panel and chopper output voltages respectively;  $I_{pv}$  and  $I_{out}$  are PV panel and chopper output currents respectively; and  $D$  is the switching period's duty cycle.



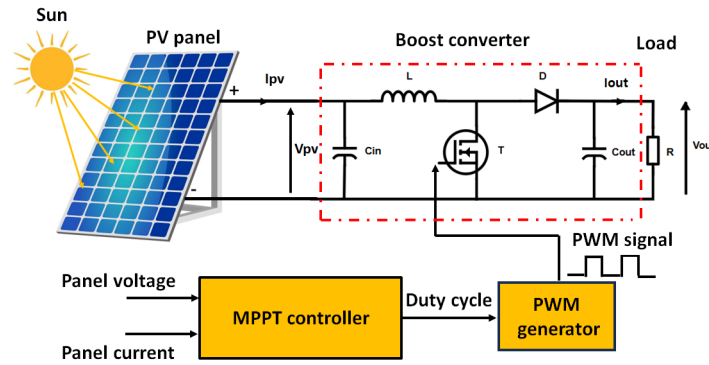


Figure 12. PV system diagram

Table 2. PV panel electrical parameters under standard test conditions (STC)

Electrical parameter	Theoretical value
Maximal power ( $P_{max}$ )	260 W
Voltage at maximal power ( $V_{mpp}$ )	30.6 V
Current at maximal power ( $I_{mpp}$ )	8.5 A
Open circuit voltage ( $V_{oc}$ )	37.8 V
Short circuit current ( $I_{sc}$ )	8.8 A
Temperature coefficient of $V_{oc}$	$-3.564.10^{-1}\%/^{\circ}C$
Temperature coefficient of $I_{sc}$	$5.3727.10^{-2}\%/^{\circ}C$

Table 3. Boost converter's electrical parameters

Electrical parameter	Value
Input capacitor ( $C_{in}$ )	1 mF
Output capacitor ( $C_{out}$ )	220 $\mu$ F
Inductor ( $L$ )	18 mH
Switching frequency $f$	10 KHz

## 5. RESULTS AND DISCUSSION

Simulation of the PV system model has been performed on MATLAB-Simulink software, as shown in Figure 13. Simulation is run for all five MPPT control methods developed in this work: P&O, IC, FL, ANNs, and ANFIS. The P&O, IC, and FL controllers have the same inputs voltage  $V_{pv}$  and current  $I_{pv}$ , whereas ANNs and ANFIS controllers have inputs are irradiation  $G$  and temperature  $T$ . To evaluate the performances of the various controllers, the model is simulated and tested under various weather conditions, as shown in Figure 14. During time interval  $[0, 0.5]$  s the PV generator is operated at standard weather test conditions ( $G = 1000$   $W/m^2$ ,  $T=25^{\circ}C$ ). The temperature remains constant during the interval  $[0.5, 1]$  s, while irradiance decreases to  $600$   $W/m^2$ . The drop continues at  $300$   $W/m^2$  for  $32^{\circ}C$  at interval  $[1, 1.5]$  s. At temperature  $30^{\circ}C$ , irradiance increases to  $700$   $W/m^2$  during  $[1.5, 2]$  s. In the interval  $[2, 2.5]$  s the irradiance decreases to  $500$   $W/m^2$  at  $27^{\circ}C$ . Lastly, the temperature remains constant as irradiance increases to  $900$   $W/m^2$  during  $[2.5, 3]$  s. To verify the comparative performance for a more formal tone between the five controllers, simulation results illustrated in Figure 15 are analyzed below.

Simulation results of power provided by PV panels under different weather conditions are shown in Figure 15. All five MPPT controllers demonstrated their capacity to track the maximum power point (MPP) under sudden changes in irradiance and temperature. The power outputs consistently converged toward theoretical maximum values, with varying levels of efficiency and stability across the different algorithms. High oscillations are observed for P&O control followed by the IC method, reduced by FL control, and almost zero for ANNs and ANFIS techniques. Tracking time is the longest for the IC method, which is its main drawback, whereas all other methods have comparable response times. Numerical simulation values for maximum power are given in Table 4. PV generator efficiency, power overshoot, power undershoot, and ripple around maximum power point (MPP) are also mentioned. PV generator operates under theoretical MPPT for all tested methods

(P&O, IC, FL, ANNs, and ANFIS) with acceptable error levels, lowest errors are found for ANNs and ANFIS methods. Efficiency is above 99% for all methods studied in this work. No overruns are observed, and underruns are reasonable for all orders. The FL, ANNs, and ANFIS intelligent methods are the closest to the optimum. The ANNs and ANFIS techniques have very close results, the best being ANFIS. Numerical ripple values of P&O control are greatest among other techniques, reaching 0.23 W. ANNs and ANFIS approaches have the lowest ripple values, ranging between 0.0013 W and 0.005 W for ANNs and from 0.001 W to 0.007 W for ANFIS.

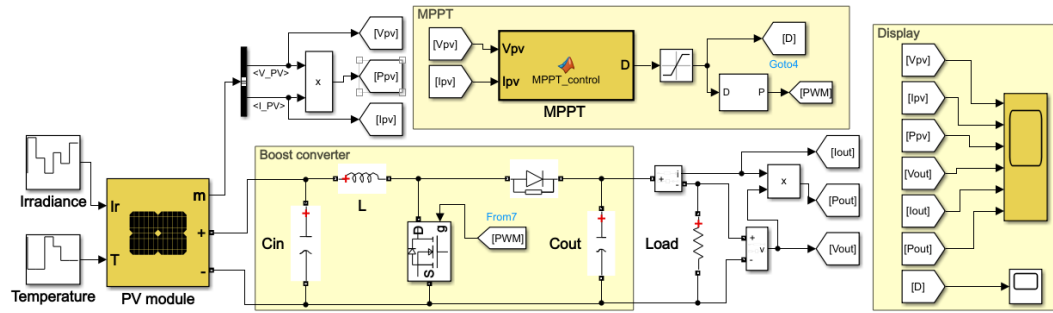


Figure 13. PV system model simulation

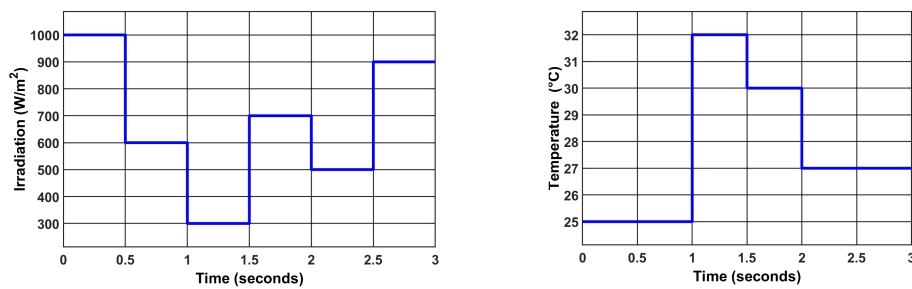


Figure 14. Inputs weather conditions for PV generator

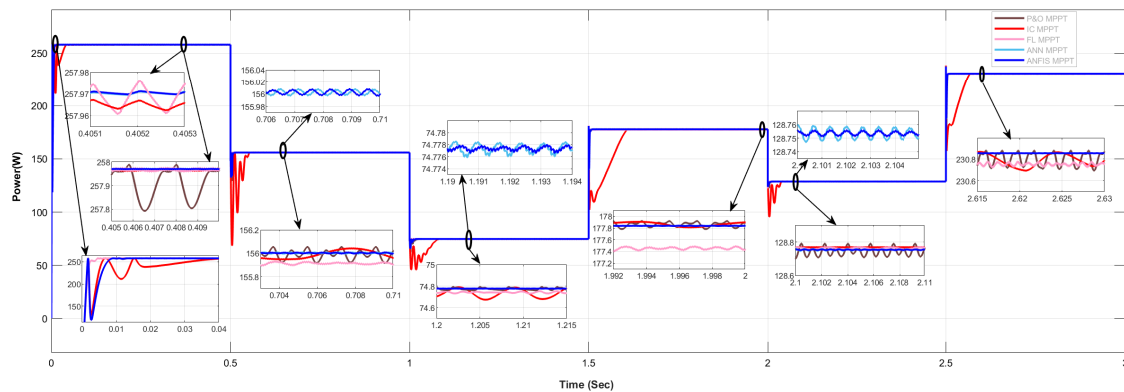


Figure 15. Output power for algorithms MPPT proposed under various climatic conditions

Classical control methods offer contrasting advantages for a more precise description: P&O is characterized by high oscillations, while its response time is lower than IC's. FL combines the two advantages of low oscillations and comparable response time to PO. In this study, ANNs and ANFIS approaches have the lowest response times, and values are very close. ANFIS is the best for this criterion. Results are given in Table 5. PV panel electrical voltage and current waveforms at maximum power point (MPP) are shown in Figure 16. Numerical results are close to theoretical results for  $I_{mpp}$  current and  $V_{mpp}$  panel voltage under different

weather conditions, as shown in Table 6. The highest oscillations are found for the P&O method, improved with the IC technique. FL and IC current oscillations are close. The lowest current and voltage ripples are reported by ANNs and ANFIS.

Intelligent approaches (ANNs and ANFIS) have proven robust MPPT control for PV systems compared to conventional methods for a more formal tone. Moreover, these AI techniques for better clarity are simple in implementation, requiring only two voltage and current sensors. FL requires improvement to reduce system computation time. On the other hand, AI techniques are more complex to implement, Table 7 summarizes the main characteristics relating to the complexity of the techniques studied. FL demands a long computation time due to software complexity, and requires a solid mastery of PV parameters; ANNs and ANFIS require a database of the pairing (G, T), a learning system, plus sensors for voltage, temperature, and irradiance.

Table 4. MPPT simulation results at different weather conditions

Atmospheric conditions	$G(W/m^2)$	1000	600	300	700	500	900
	T(°C)	25	25	32	30	27	27
$P_{max}(W)$	(Theoretical value)	258	156.04	74.78	177.88	128.77	230.86
P&O	$P_{MPPT}(W)$	257.87	156	74.775	177.83	128.75	230.78
	Efficiency(%)	99.94	99.97	99.99	99.97	99.98	99.96
	MPPT Error(%)	0.050	0.025	0.006	0.028	0.015	0.034
	Overshoot(W)	0	0	0	0	0	0
	Undershoot(W)	0.13	0.04	0.005	0.03	0.05	0.08
	Ripple(W)	0.19	0.13	0.027	0.106	0.097	0.23
IC	$P_{MPPT}(W)$	257.965	155.95	74.73	177.85	128.768	230.79
	Efficiency(%)	99.98	99.94	99.93	99.98	99.99	99.96
	MPPT Error(%)	0.013	0.057	0.066	0.001	0.001	0.030
	Overshoot(W)	0	0	0	0	0	0
	Undershoot(W)	0.035	0.09	0.05	0.030	0.002	0.070
	Ripple(W)	0.11	0.12	0.12	0.009	0.001	0.128
FL	$P_{MPPT}(W)$	257.967	155.9	74.74	177.45	128.76	230.75
	Efficiency(%)	99.98	99.91	99.94	99.75	99.99	99.95
	MPPT Error(%)	0.012	0.089	0.053	0.241	0.007	0.047
	Overshoot(W)	0	0	0	0	0	0
	Undershoot(W)	0.033	0.14	0.04	0.43	0.01	0.11
	Ripple(W)	0.013	0.04	0.02	0.09	0.004	0.05
ANN	$P_{MPPT}(W)$	257.97	156	74.777	177.83	128.753	230.852
	Efficiency(%)	99.98	99.97	99.99	99.97	99.98	99.99
	MPPT Error(%)	0.011	0.025	0.004	0.028	0.013	0.003
	Overshoot(W)	0	0	0	0	0	0
	Undershoot(W)	0.03	0.04	0.003	0.05	0.017	0.008
	Ripple(W)	0.0013	0.005	0.005	0.002	0.003	0.0016
ANFIS	$P_{MPPT}(W)$	257.97	156	74.777	177.836	128.753	230.853
	Efficiency(%)	99.98	99.97	99.99	99.97	99.98	99.99
	MPPT Error(%)	0.011	0.025	0.004	0.024	0.013	0.003
	Overshoot(W)	0	0	0	0	0	0
	Undershoot(W)	0.03	0.04	0.003	0.044	0.017	0.007
	Ripple(W)	0.0012	0.004	0.005	0.001	0.007	0.0014

Table 5. Results of tracking and falling time at MPP under various weather conditions

Atmospheric conditions	$G(W/m^2)$	1000	600	300	700	500	900
	T(°C)	25	25	32	30	27	27
P&O	Tracking time(ms)	14.19	12.91	31.85	14	14.79	12.18
	Falling time(ms)	0	0	0	0	0	0
IC	Tracking time(ms)	43.92	54.3	82.24	110.96	39.2	69.99
	Falling time(ms)	0	0	0	0	0	0
FL	Tracking time(ms)	10.03	14.8	30.46	12.70	15.83	10.01
	Falling time(ms)	0	0	0	0	0	0
ANNs	Tracking time(ms)	13.53	19.02	20.84	12.65	12.65	9.95
	Falling time(ms)	0	0	0	0	0	0
ANFIS	Tracking time(ms)	13.5	18.50	20.58	12.59	12.61	9.18
	Falling time(ms)	0	0	0	0	0	0

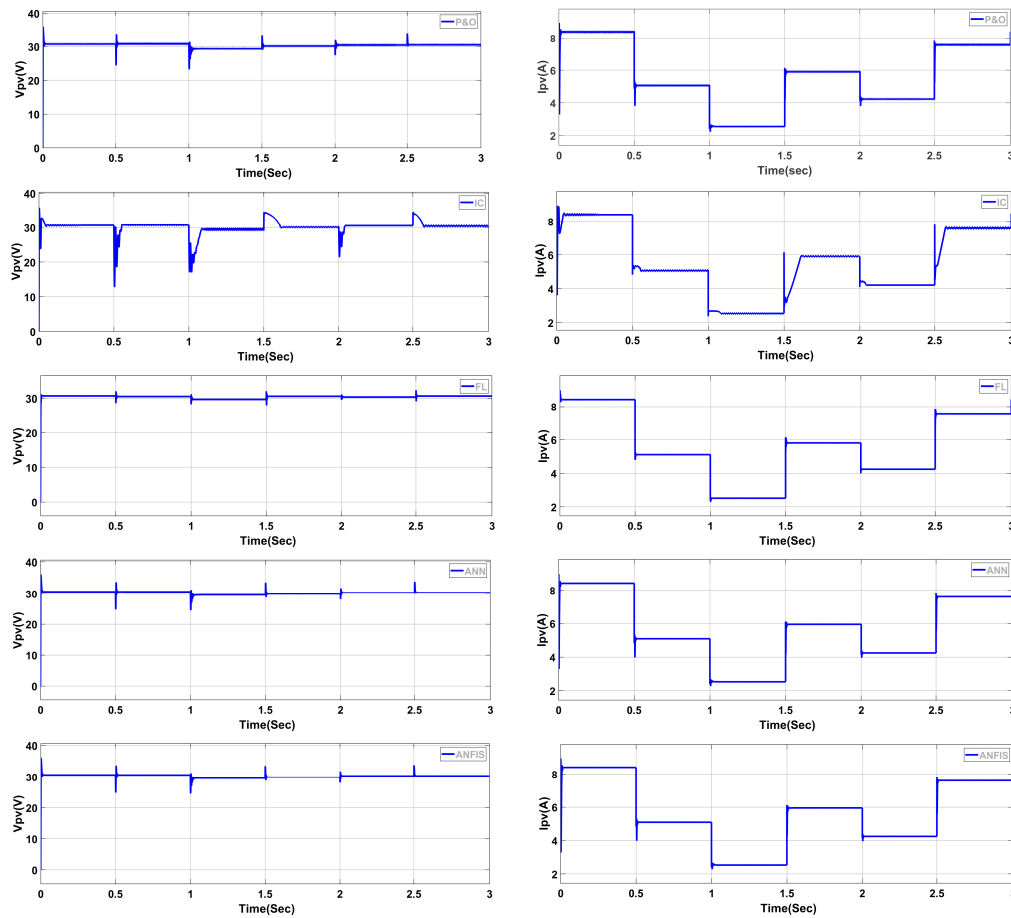


Figure 16. GPV voltage and current waveforms for proposed approaches

Table 6. Results of  $V_{pv}$  and  $I_{pv}$  at MPP under various weather conditions

Atmospheric conditions	$G(W/m^2)$	1000	600	300	700	500	900	
	T(°C)	25	25	32	30	27	27	
P&O	$V_{mpp}(V)$	Theoretical value	30.6	30.79	29.52	29.97	30.53	30.37
	$I_{mpp}(A)$	Theoretical value	8.5	5.06	2.53	5.94	4.21	7.6
	$V_{pv}(V)$		30.71	30.80	29.39	30.13	30.45	30.47
	$I_{pv}(A)$		8.39	5.06	2.54	5.90	4.22	7.56
	Voltage ripple(V)		0.29	0.41	0.23	0.35	0.39	0.30
IC	Current ripple(A)		0.09	0.07	0.02	0.07	0.04	0.09
	$V_{pv}(V)$		30.66	30.79	29.45	30.12	30.54	30.41
	$I_{pv}(A)$		8.41	5.06	2.53	5.9	4.21	7.58
	Voltage ripple(V)		0.03	0.05	0.07	0.03	0.01	0.05
	Current ripple(A)		0.007	0.008	0.06	0.07	0.002	0.12
FL	$V_{pv}(V)$		30.65	30.49	29.67	30.54	30.35	30.62
	$I_{pv}(A)$		8.41	5.11	2.51	5.81	4.24	7.53
	Voltage ripple(V)		0.018	0.071	0.05	0.051	0.042	0.042
	Current ripple(A)		0.007	0.009	0.005	0.012	0.006	0.008
	$V_{pv}(V)$		30.64	30.62	29.56	29.88	30.32	30.33
ANNs	$I_{pv}(A)$		8.41	5.09	2.52	5.95	4.24	7.60
	Voltage ripple(V)		0.003	0.008	0.004	0.004	0.003	0.002
	Current ripple(A)		0.001	0.001	0.001	0.001	0.001	0.001
	$V_{pv}(V)$		30.63	30.62	29.56	29.88	30.32	30.33
	$I_{pv}(A)$		8.41	5.09	2.529	5.951	4.246	7.609
ANFIS	Voltage ripple(V)		0.0026	0.006	0.004	0.004	0.0029	0.0019
	Current ripple(A)		0.0009	0.0007	0.0006	0.0009	0.0009	0.0007

Table 7. Comparative features of different MPPT strategies

MPPT algorithms	Algorithm complexity	Analog or digital	PV array dependency	Sensed parameters
P&O	Low	Both	No	Voltage, current
IC	Medium	Digital	No	Voltage, current
FL	Medium	Digital	Yes	Voltage, current
ANNs	High	Digital	Yes	Irradiance, temperature, and voltage
ANFIS	High	Digital	Yes	Irradiance, temperature, and voltage

## 6. CONCLUSION

This study investigates the performance of maximum power point tracking (MPPT) control in a photovoltaic (PV) system subjected to diverse weather patterns. Five MPPT algorithms are evaluated: Perturb and Observe (PO), incremental conductance (IC), fuzzy logic (FL), artificial neural networks (ANNs), and adaptive neuro-fuzzy inference system (ANFIS). The proposed PV system model, built within MATLAB Simulink software, comprises a PV generator, resistor load, and DC/DC boost chopper driven by an MPPT controller. Simulation results confirm that intelligent approaches like ANNs and ANFIS significantly outperform classical methods. While P&O and IC offer simplicity, they struggle with oscillations and slower response times. ANNs and ANFIS, on the other hand, provide faster tracking and more stable operation, making them suitable for modern PV systems. Future research could focus on optimizing these intelligent methods for real-world applications, further enhancing PV system efficiency.




## REFERENCES

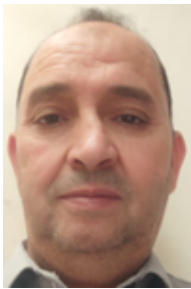
- [1] M. E. Başoğlu, "An approximate short circuit strategy for transient MPPT performance of uniformly irradiated photovoltaic modules," *Journal of Electrical and Computer Engineering*, vol. 7, no. 1, pp. 88-93, Jan. 2019, doi: 10.17694/bajece.499932.
- [2] C. R. Çırak and H. Çalık, "Hotspots in maximum power point tracking algorithms for photovoltaic systems – A comprehensive and comparative review," *Engineering Science and Technology, an International Journal*, vol. 43, pp. 101436, Jul. 2023, doi: 10.1016/j.jestech.2023.101436.
- [3] D. Baimel, S. Tapuchi, Y. Levron, and J. Belikov, "Improved fractional open circuit voltage MPPT methods for PV systems," *Electronics*, vol. 8, no. 321, pp. 1-20, Mar. 2019, doi: 10.3390/electronics8030321.
- [4] F. Çakmak, Z. Aydoğmuş, and M. R. Tür, "Analysis of open circuit voltage MPPT method with analytical analysis with perturb and observe (P&O) MPPT method in PV systems," *Electric Power Components and Systems*, vol. 52, no. 9, pp. 1528–1542, May. 2024, doi: 10.1080/15325008.2023.2296958.
- [5] A. Nadeem, H. A. Sher, A. F. Murtaza, and N. Ahmed, "Online current-sensorless estimator for PV open circuit voltage and short circuit current," *Solar Energy*, vol. 213, pp. 198-210, Jan. 2021, doi: 10.1016/j.solener.2020.11.004.
- [6] A. G. Abdullah, M. S. Aziz, and B. A. Hamad, "Comparison between neural network and P&O method in optimizing MPPT control for photovoltaic cell," *International Journal of Electrical and Computer Engineering*, vol. 10, no. 5, pp. 5083-5092, Oct. 2020, doi: 10.11591/ijece.v10i5.pp5083-5092.
- [7] A. Hassani, M. Maamoun, R. Tadriss, and A. Nesba, "A new high speed and accurate FPGA-based maximum power point tracking method for photovoltaic systems," *International Journal of Power Electronics and Drive Systems*, vol. 8, no. 3, pp. 1335–1344, Sept. 2017, doi: 10.11591/ijpeds.v8.i3.pp1335-1344.
- [8] M. A. Elgendy, B. Zahawi, and D. J. Atkinson, "Assessment of the incremental conductance maximum power point tracking algorithm," *IEEE Transactions on Sustainable Energy*, vol. 4, no. 1, pp. 108–117, Jan. 2013, doi: 10.1109/TSTE.2012.2202698.
- [9] S. Z. Mirbagheri, S. Mekhilef, and S. M. Mirhassani, "MPPT with Inc. Cond method using conventional interleaved boost converter," *Energy Procedia*, vol. 42, pp. 24-32, 2013, doi: 10.1016/j.egypro.2013.11.002.
- [10] L. Shang, H. Guo, and W. Zhu, "An improved MPPT control strategy based on incremental conductance algorithm," *Protection and Control of Modern Power Systems*, vol. 5, no. 2, pp. 1-8, Apr. 2020, doi: 10.1186/s41601-020-00161-z.
- [11] S. Ait. El. Ouahab, F. Bakkali, A. Amghar, H. Sahah, El. Mentaly, and L. El. Mahfoud, "Design and implementation of temperature-parametric for maximum power point tracking of photovoltaic systems: Experimental validation using PI controller," *Computers and Electrical Engineering*, vol. 120, Dec. 2024, p. 109707, doi: 10.1016/j.compeleceng.2024.109707.
- [12] M. Lasheen and M. Abdel-Salam, "Maximum power point tracking using Hill Climbing and ANFIS techniques for PV applications: A review and a novel hybrid approach," *Energy Conversion and Management*, vol. 171, pp. 1002-1019, Sept. 2018, doi: 10.1016/j.enconman.2018.06.003.
- [13] J. Shi, W. Zhang, Y. Zhang, F. Xue, and T. Yang, "MPPT for PV systems based on a dormant PSO algorithm," *Electric Power Systems Research*, vol. 123, pp. 100-107, Jun. 2015, doi: 10.1016/j.epsr.2015.02.001.
- [14] S. K. G., S. Kinattingal, S. P. Simon, and P. S. R. Nayak, "MPPT in PV systems using ant colony optimisation with dwindling population," *IET Renewable Power Generation*, vol. 14, no. 7, pp. 1105–1112, Mar. 2020, doi: 10.1049/iet-rpg.2019.0875.
- [15] A. M. Eltamaly, H. M. H. Farh, and M. S. Al-Saud, "Grade point average assessment for metaheuristic GMPP techniques of partial shaded PV systems," *IET Renewable Power Generation*, vol. 13, no. 8, pp. 1215-1231, Mar. 2019, doi: 10.1049/iet-rpg.2018.5336.
- [16] M. Agdam, S. Assalaoui, E. Aitiaz, D. B. Hmamou, Y. E. Idrissi, S. Lidaighbi, S. Driss, and M. Elyagouti, "A novel algorithm MPPT controller based on the herd horse optimization for photovoltaic systems under partial shadow conditions," *Engineering Research Express*, vol. 6, no. 3, p. 035308, Jul. 2024, doi: 10.1088/2631-8695/ad5f16.




- [17] A. M. Eltamaly, "An improved cuckoo search algorithm for maximum power point tracking of photovoltaic systems under partial shading conditions," *Energies*, vol. 14, no. 4, p. 953, Feb. 2021, doi: 10.3390/en14040953.
- [18] A. K. Sharma, R. K. Pachauri, S. Choudhury, A. F. Minai, M. A. Alotaibi, H. Malik, and F. P. G. Márquez, "Role of metaheuristic approaches for implementation of integrated MPPT-PV systems: A comprehensive study," *Mathematics*, vol. 11, no. 2, pp. 269, Jan. 2023, doi: 10.3390/math11020269.
- [19] K. H. Chalok, M. F. N. Tajuddin, T. S. Babu, S. M. Ayob, T. Sutikno, and J. Belikov, "Optimal extraction of photovoltaic energy using fuzzy logic control for maximum power point tracking technique," *International Journal of Power Electronics and Drive Systems*, vol. 11, no. 3, pp. 1628–1639, Sept. 2020, doi: 10.11591/ijpeds.v11.i3.pp1628-1639.
- [20] M. S. A. Cheikh, C. Larbes, G. F. T. Kebir, and A. Zerguerras, "Maximum power point tracking using a fuzzy logic control scheme," *Journal of Renewable Energies*, vol. 10, no. 3, pp. 387–395, Sept. 2007, doi: 10.54966/jreen.v10i3.771.
- [21] L. Farah, A. Haddouche, and A. Haddouche, "Comparison between proposed fuzzy logic and anfis for MPPT control for photovoltaic system," *International Journal of Power Electronics and Drive Systems*, vol. 11, no. 2, pp. 1065–1073, Jun. 2020, doi: 10.11591/ijpeds.v11.i2.pp1065-1073.
- [22] K. Boudaraia, H. Mahmoudi, and A. Abbou, "MPPT design using artificial neural network and backstepping sliding mode approach for photovoltaic system under various weather conditions," *International Journal of Intelligent Engineering and Systems*, vol. 12, no. 6, pp. 177–186, Sept. 2019, doi: 10.22266/ijies2019.1231.17.
- [23] S. Messalti, A. Harrag, and A. Loukriz, "A new variable step size neural networks MPPT controller: Review, simulation and hardware implementation," *Renewable and Sustainable Energy Reviews*, vol. 68, no. 1, pp. 221–233, Feb. 2017, doi: 10.1016/j.rser.2016.09.131.
- [24] F. Sedaghati, A. Nahavandi, M. A. Badamchizadeh, S. Ghaemi, and M. A. Fallah, "PV maximum power-point tracking by using artificial neural network," *Mathematical Problems in Engineering*, vol. 2012, no. 1, p. 10, Mar. 2012, doi: 10.1155/2012/506709.
- [25] W. S. Pambudi, R. A. Firmansyah, Y. A. Prabowo, T. Suheta, and F. Fathammubina, "Designing ANFIS controller for MPPT on photovoltaic system," *Jurnal Rekayasa Elektrika*, vol. 19, no. 2, pp. 64–70, Jun. 2023, doi: 10.17529/jre.v19i2.23394.
- [26] D. T. Nguyen, D. H. Nguyen, V. T. Le, and T. T. Hoang, "An explicit approach to simulate the five-parameter model for PV panels under various conditions," *Journal of Science and Engineering*, vol. 1, no. 2, pp. 6–13, 2020, doi: 10.34436/sjse.1.2.6.
- [27] R. Kumar, and S. K. Singh, "Solar photovoltaic modeling and simulation: As a renewable energy solution," *Energy Reports*, vol. 4, pp. 701–712, Nov. 2018, doi: 10.1016/j.egyr.2018.09.008.
- [28] N. Yahyaoui, S. Mansouri, A. G. Al-Sehemi, A. Dere, A. Al-Ghamdi, and F. Yakuphanoglu, "Electrical characterization of silicon PV-cell: modeling," *Applied Physics*, vol. 130, no. 6, p. 379, May 2024, doi: 10.1007/s00339-024-07523-6.
- [29] X. H. Nguyen, and M. P. Nguyen, "Mathematical modeling of photovoltaic cell/module/arrays with tags in MATLAB/Simulink," *Environmental Systems Research*, vol. 4, no. 1, pp. 1–13, Dec. 2015, doi: 10.1186/s40068-015-0047-9.
- [30] M. Slimi, A. Boucheta, and B. Bouchiba, "Maximum power control for photovoltaic system using intelligent strategies," *International Journal of Power Electronics and Drive Systems*, vol. 10, no. 1, pp. 423–432, Mar. 2019, doi: 10.11591/ijpeds.v10.i1.pp423-432.
- [31] I. Yadav, S. K. Maurya, and G. K. Gupta, "A literature review on industrially accepted MPPT techniques for solar PV system," *International Journal of Electrical and Computer Engineering*, vol. 10, no. 2, pp. 2117–2127, Apr. 2020, doi: 10.11591/ijece.v10i2.pp2117-2127.
- [32] U. Yilmaz, A. Kircay, and S. Borekci, "PV system fuzzy logic MPPT method and PI control as a charge controller," *Renewable and Sustainable Energy Reviews*, vol. 81, no. 1, pp. 994–1001, Jan. 2018, doi: 10.1016/j.rser.2017.08.048.
- [33] S. Srinivasan, R. Tiwari, M. Krishnamoorthy, M. P. Lalitha, and K. K. Raj, "Neural network based MPPT control with reconfigured quadratic boost converter for fuel cell application," *International Journal of Hydrogen Energy*, vol. 46, no. 9, pp. 6709–6719, Feb. 2021, doi: 10.1016/j.ijhydene.2020.11.121.
- [34] S. A. Touil, N. Boudjerda, A. Boubakir, and K. E. K. Drissi, "A sliding mode control and artificial neural network based MPPT for a direct grid-connected photovoltaic source," *Asian Journal of Control*, vol. 21, no. 4, pp. 1892–1905, Jan. 2019, doi: 10.1002/asjc.2007.
- [35] Y. E. A. Idrissi, K. Assalaou, L. Elmahni, and E. Aitiaz, "New improved MPPT based on artificial neural network and PI controller for photovoltaic applications," *International Journal of Power Electronics and Drive Systems*, vol. 13, no. 3, pp. 1791–1801, Sep. 2022, doi: 10.11591/ijpeds.v13.i3.
- [36] M. Ahmed, I. Harbi, R. Kennel, and M. Abdelrahem, "Predictive fixed switching maximum power point tracking algorithm with dual adaptive step-size for PV systems," *Electronics*, vol. 10, no. 24, p. 3109, Dec. 2021, doi: 10.3390/electronics10243109.
- [37] A. Garcés-Ruiz, W. Gil-González, and O. D. Montoya, "Stability analysis for an ad-hoc model predictive control in DC/DC converters with a constant power load," *Results in Engineering*, vol. 22, p. 102262, Jun. 2024, doi: 10.1016/j.rineng.2024.102262.

## BIOGRAPHIES OF AUTHORS






**Meriem Boudouane**    graduated in electronics from Al Idrissi Technical High School. She then obtained a University Diploma of Technology (DUT) in Electrical Engineering from the Higher School of Technology (EST) Agadir, A fundamental degree in Physical Sciences, and a Master's degree in Materials Engineering and Renewable Energy at the Physics Department of the Faculty of Science, University Ibn Zohr Agadir, Morocco. She is currently working on her research into the management and optimization of microgrid energy flows. She can be contacted at email: meriem-prof@gmail.com.






**Lahoussine Elmahni**    was born in Agadir, Morocco in 1968; Professor (1993) in electrical engineering at faculty of science with bachelor (1989) in electronics in higher normal school of technology (ENSET), Rabat and a post graduate degree in (2008), of energy and environment in the National School of Applied Sciences (ENSA) of Agadir, His research is focused on Smart Grid, electric vehicles, demand response, energy efficiency, renewable energy integration, energy storage and distributed resources. He can be contacted at email: l.elmahni@uiz.ac.ma.



**Rachid Zriouile**    was born in Agadir, Morocco, in 1992. In 2012, he obtained a University Diploma in Technology, option Electrical Engineering, from the High School of Technology in Agadir. In 2015, he got an engineering diploma in Electrotechnics and Industrial Electronics from the Faculty of Sciences and Techniques of Beni Mellal. His research focuses on renewable energy. Currently, he is working on his doctoral thesis titled "Energy optimization of a system based on renewable energies and management of its integration into the electrical grid". He can be contacted at email: rachid.zriouile@edu.uiz.ac.ma.



**Soufyane Ait El Ouahab**    received his Lic degree in Electronics and Systems of Communication from Ibn Zohr University. Hold a Master's degree in Systems and Telecommunication from the Faculty of Sciences, Ibn Zohr University, Agadir, Morocco. Currently, a Ph.D. student in Electronics and Renewable Energies at the Department of Physics, Laboratory of Metrology and Information Processing Lab, Ibnou Zohr University. His main research interests include Contribution to the improvement of MPPT techniques associated with a set of PV generators under shade. He can be contacted at email: soufyane.aitelouahab@edu.uiz.ac.ma.